ACS APPLIED MATERIALS & INTERFACES
Research Article
www.acsami.org

Li^+-Conductive Polymer-Embedded Nano-Si Particles as Anode Material for Advanced Li-ion Batteries

Yao Chen,[†] Shi Zeng,[†] Jianfeng Qian,[†] Yadong Wang,[‡,*] Yuliang Cao,[†] Hanxi Yang,[†] and Xinping Ai*[,†]

[†]Hubei Key Lab. of Electrochemical Power Sources, Department of Chemistry, Wuhan University, Wuhan 430072, China
[‡]State Key Laboratory of Advanced Technology for Materials Synthesis and Processing, Wuhan University of Technology, Wuhan 430070, China

Supporting Information

ABSTRACT: Si has been considered as a promising alternative anode for next-generation lithium ion batteries (LIBs), but the commercial application of Si anodes is still limited due to their poor cyclability. In this paper, we propose a new strategy to enhance the long-term cyclability of Si anode by embedding nano-Si particles into a Li^+-conductive polymer to form a Si/polymer composite with core-shell structure, in which nano-Si cores act as active Li-storage phase and the polymeric matrix serves not only as a strong buffer to accommodate the volume change, but also as a protection barrier to prevent the direct contact of Si surface with electrolyte, so as to maintain the mechanical integrity of Si anode and suppress the repeated destruction and construction of solid electrolyte interphase (SEI) on the Si surface. To realize this strategy, we synthesize a Si/PPP (polyparaphenylene) composite simply by ball-milling the Si nanoparticles with PPP polymer that has n-doping activity. Our experimental results demonstrate that the thus-prepared Si/PPP composite exhibits a high capacity of 3184 mA h g^{-1} with an initial coulombic efficiency of 78%, an excellent rate capability with a considerably high capacity of 1670 mA h g^{-1} even at a very high rate of 16 A g^{-1}, and a long-term cyclability with 60% capacity retention over 400 cycles, showing a great prospect for battery application. In addition, this structural design could be adopted to other Li-storable metals or alloys for developing cycle-stable anode materials for Li-ion batteries.

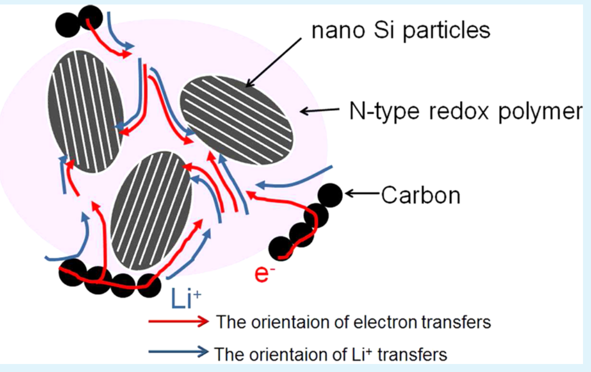

KEYWORDS: *lithium-ion batteries, anode material, silicon, Li^+-conductive polymer, polyparaphenylene (PPP)*

■ INTRODUCTION

Developing advanced lithium-ion batteries (LIBs) with substantially enhanced energy density and safety is of great technological importance for large scale energy storage applications, such as in electrical vehicles, smart grid, and renewable power stations.[1−5] In this technological development, Si has attracted particular interest as a new anode material, because of its appropriate lithiation potential (+ 0.2 V, vs Li^+/Li) and extremely high theoretical Li-storage capacity of 4200 mA h g^{-1} ($Li_{4.4}Si$), which is more than ten times higher than the theoretical capacity of the graphite anode used in current Li-ion technology.[6−8] However, commercial development of Si anodes is less successful mainly due to their poor cyclability, which is resulted from the huge volumetric changes (∼300%) during lithium insertion/extraction cycles. Such an enormous volume change brings about two severe problems for Li-ion battery applications. One is the degradation of the mechanical integrity of the Si anode, simply because the drastic volume expansion and contraction at cycling would cause the fracture and pulverization of Si particles, leading to the loss of electrical contact and the gradual deactivation of the active materials. The other is the continuous change in the structure and morphology of the solid electrolyte interphase (SEI) on the Si surface. Because the Si particles are continuously fractured and pulverized at the impact of the volume change, the SEI film on the Si surface has to be reconstructed during every cycle. The repeated construction and destruction of the SEI film affect adversely the cycling performance of the Si anode at least in three aspects: the first one is the continuous decomposition of the electrolyte for formation of new SEI films, which must lead to a low coulombic efficiency and eventually an exhaustion of Li ions and electrolyte. Secondly, the continuous growth of electronically insulating SEI film can cause electric disconnection between the electrode collector and anode materials. Furthermore, the thickened SEI film imposes a high resistance to Li insertion reaction.

To solve these problems, a large variety of nanoarchitectures has been proposed to buffer the mechanical stress of lithiated Si anodes, so as to improve the cycling stability.[9−14] Previous studies have demonstrated that the mechanical degradation of Si particles could be effectively depressed in well-designed Si nanostructures such as porous Si nanowires,[15−17] nano-

Received: December 9, 2013
Accepted: January 27, 2014
Published: January 27, 2014

spheres[18−22] and nanotubes.[23−25] However, because of the instability of the SEI films on the repeatedly changed surfaces of the nano-Si particles, the long-term cycling stability of these nanoarchitectured Si anodes is still insufficient for practical use. To tackle this problem, a novel type of double walled Si nanotubes sophisticatedly designed with a stable SEI film was recently reported to have a remarkable cycle life.[23] However, this material is difficult to fabricate with complicated synthetic steps at extreme conditions.

Herein, we propose a new strategy to enhance the long-term cyclability of Si anode by embedding nano-Si particles into a Li^+-conductive polymer to form a Si/polymer composite with core-shell structure, where nano-Si cores act as an active Li-storage phase and the polymer matrix serves not only as a strong buffer to accommodate the volume change, but also as a protection barrier to prevent the direct contact of the Si surface with electrolyte. In this material design, the Si surface is embedded in the polymer and therefore separated from the electrolyte, thus avoiding the chemical erosion of electrolyte. Furthermore, the drastic volume change of active Si phase at cycling are effectively relieved by the polymer buffering matrix, so that the SEI film can be stabilized during charge-discharge cycles. To allow normal Li insertion reaction, the polymer matrix must have a n-type redox ability with acceptable electronic and ionic conductivity,[26] thus enabling fast Li^+ transport though the polymer chains to insert into/remove from the Si host during the lithithation/delithiation process. To realize this strategy, we synthesized a Si-PPP (polyparaphenylene, $-(CH_4)_n-$) composite simply by ball-milling the Si nanoparticles with the polymer matrix and tested the electrochemical behaviors of the thus-prepared Si-PPP composite.

EXPERIMENTAL SECTION

PPP was synthesized using an $AlCl_3-CuCl_2$ catalyst according to Kovacic's method.[27,28] A typical synthetic procedure was as follows: 0.78 g benzene was added dropwise into a mixture of 0.334 g anhydrous $AlCl_3$ and 0.336 g $CuCl_2$ at 0 °C. The reaction mixture was stirred at 0 °C for 1 h and then at room temperature for 24 h. The resulting mixture was filtered and the polymeric precipitate was washed several times with 18% hydrochloric acid solution and finally dried at 60 °C under vacuum for 24 h to obtain a brown powder product. The as-prepared PPP powder was further heat-treated at 400 °C in a muffle furnace for 36h.

Silicon/PPP composites were prepared simply by ball-milling the mixture of silicon nanoparticles (less than 100 nm, Alfa Aesar) and PPP with a weight ratio of 5:2 for 30 min. The milling processes were performed in a planetary ball mill (Fritsch pulverisette 23) under Ar atmosphere.

The FT-IR spectra of PPP and Si/PPP composite were recorded on a NICOLET AVATAR360 FT-IR spectrometer with KBr pellets. The crystalline structures and morphologies of the as-prepared powder samples were characterized by transmission electron microscopy (TEM, JEOL, JEM-2010-FEF).

To evaluate the electrochemical properties, we prepared the composite silicon anodes by casting the electrode slurry onto a 20 μm thick copper foil. The electrode slurry consisted of 70 wt % silicon/ppp composite, 10 wt % Ketjin Black and 20 wt % poly(acrylic acide) (PAA) as a binder, dissolved in distilled water. The electrodes were dried at 60 °C under a vacuum for overnight to remove the water. As a comparison, the pristine nano-silicon anode is also prepared in a similar way with a composition of 50 wt % nano-silicon powders, 30 wt % Ketjen Black, and 20 wt % PAA binder. The PAA binder used in this study has an average molecule weight of 240 000, purchase from Alfa Asear.

The charge/discharge experiments were performed using CR2016-type coin cells with Celgard 2400 microporous membrane as separator and a lithium disk as counter electrode. The electrolyte was 1 M $LiPF_6$ dissolved in a mixture of ethylene carbonate (EC), dimethyl carbonate (DMC) and ethyl methyl carbonate (EMC) (1:1:1, v:v:v). The cells were assembled in an argon-filled glovebox. The electrochemical performances were evaluated in a voltage range of 0.01−2.0 V on Land Battery Testing System (Wuhan Kingnuo Electronics Co., Ltd., China) at 25 °C. Cyclic voltammetry (CV) was performed on an electrochemical workstation (CHI660c, Shanghai, China) in a voltage range of 0.005-2.0 V at a scan rate of 0.1 mV s^{-1}. The electrochemical impedance measurement of the Si-PPP composite was conducted on an Impedance Measuring Unit (IM 6e, Zahner) with oscillation amplitude of 5 mV at the frequency range from 50 mHz to 100 kHz.

RESULTS AND DISCUSSION

In this work, we chose PPP polymer as the embedding matrix for the nano-Si particles mainly because, as an electroactive redox polymer, PPP has highly reversible n-doping/de-doping behaviors in the commonly used Li^+ electrolyte at a potential near that of Si lithiation and can act to mediate the transfer of Li^+ between the electrolyte and the active Si phase. According to the electrochemical redox reaction mechanism of conducting polymers, the electro-reduction of PPP corresponds to the n-doping of the Li^+ cations from electrolyte to polymer chains for charge counterbalance. Conversely, the electro-oxidation of the reduced PPP occurs through an electrochemical de-doping process simultaneously with the extraction of the Li^+ from the polymer chains. Apparently, the reversible n-doping/de-doping behaviors provide Li^+-conductivity for PPP polymer and enable Li^+ ions transport through PPP chains in/from the Si cores for the lithiation/de-lithiation reactions.

To convince the n-doping activity of PPP polymer, we measured the CV curves of a PPP electrode in Li^+ electrolyte and also the charge-discharge curves of coin-type Li-PPP half cells. As given in Figure 1, the CV curves from the PPP electrode have a pair of well-defined redox peaks at low potential region of 1.0−0.2 V, which resemble very much the CV features of Li insertion reaction on the carbonaceous anodes, suggesting reversible Li^+ doping/de-doping reactions in the PPP chains. The charge/discharge curves shown in the inset of Figure 1 further confirm the availability of the PPP polymer

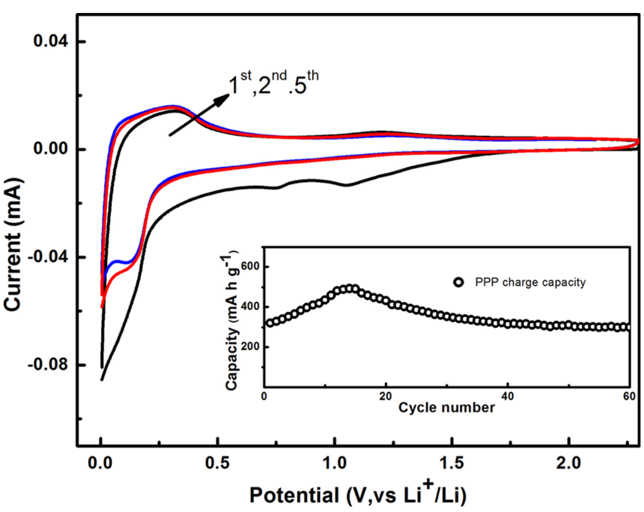

Figure 1. CV curves of the PPP polymer in 1 M $LiPF_6$/EC-DMC-EMC electrolyte. The inset displays the cycling performance of the PPP electrode.

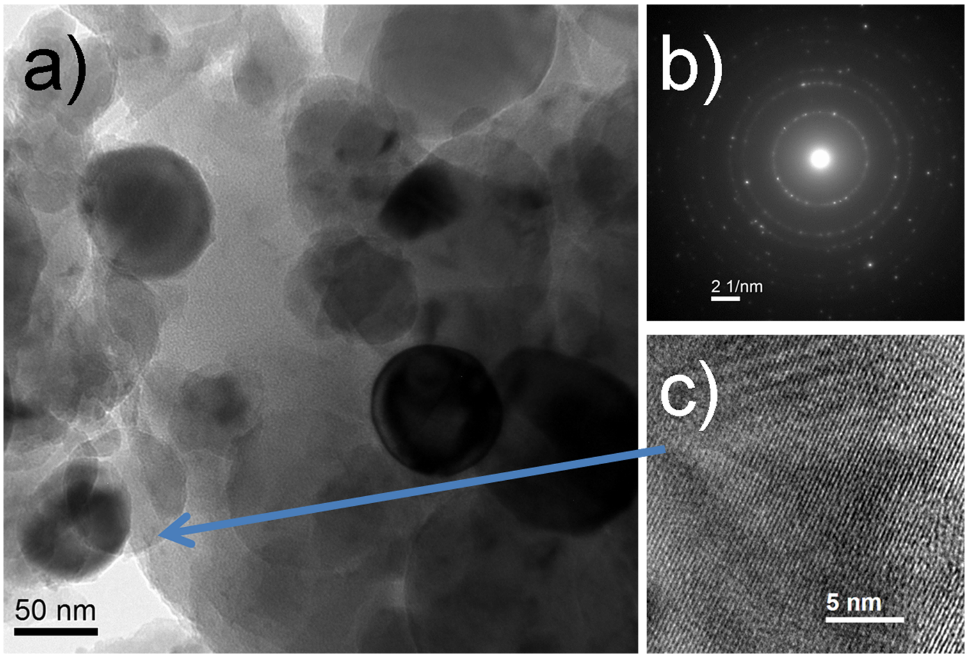

Figure 2. (a) TEM image, (b) electron diffraction patteren, and (c) HRTEM image of the Si-PPP composite.

as an n-dopable anode with a stable Li-storage capacity of ∼400 mA h g^{-1}. According to the 20 wt % PPP content in the composite, the calculated contribution of the PPP polymer to the total capacity of the composite is ∼100 mA h g^{-1}.

Figure 2 shows the morphological feature of the Si-PPP composite. As is shown in Figure 2a, the composite consists of spherelike particles with a core-shell structure. The inner cores are composed of Si nanoparticles with average size of ∼80 nm and the outer shell is consisted of PPP polymer. The electron diffraction image in Figure 2b demonstrates a cubic symmetry diffraction spot pattern, revealing that the Si particles still exist in a crystalline state after ball-milling treatment. High-resolution TEM image from a single grain in Figure 2c shows well-defined lattice fringes of 0.31 nm, corresponding to the d-spacing value of the (111) plane of the cubic Si phase. The infrared spectrum of the as-prepared composite sample showed clearly all the strong characteristic vibrations of PPP rings (see Figure S1 in the Supporting Information). These results demonstrate that the brittle Si particles have been successfully embedded into the flexible polymer matrix to form a core-shelled Si-PPP composite during ball-milling. Apparently, this structure allows for the growth of a stable SEI film on the outer surface of the polymer shell and can prevent the repeated construction and destruction of the SEI on the Si surface during cycling, so as to enhance the long-term cyclability of Si anode.

The cyclic voltammograms (CV) and charge/discharge curves of the Si-PPP composite electrode are shown in Figure 3. As displayed in Figure 3a, a broad reduction band at ∼0.8 V usually observed for the SEI film formation on the Si surface appears very weak, almost indiscernible in the initial cathodic scan, suggesting that the decomposition of electrolyte for building SEI film is greatly depressed on the Si-PPP composite. Nevertheless, there is still a sharp and strong cathodic peak appearing at a lithiation potential of 0.2 V, indicating that the PPP shell did not affect the Li^+-insertion into the Si phase. After the initial cycle, two pairs of reversible redox peaks appear at 0.03/0.33 V and 0.21/0.50 V respectively, featuring a two stepped alloying reaction of Si with Li^+ ions as usually observed from Si-based anodes.[29]

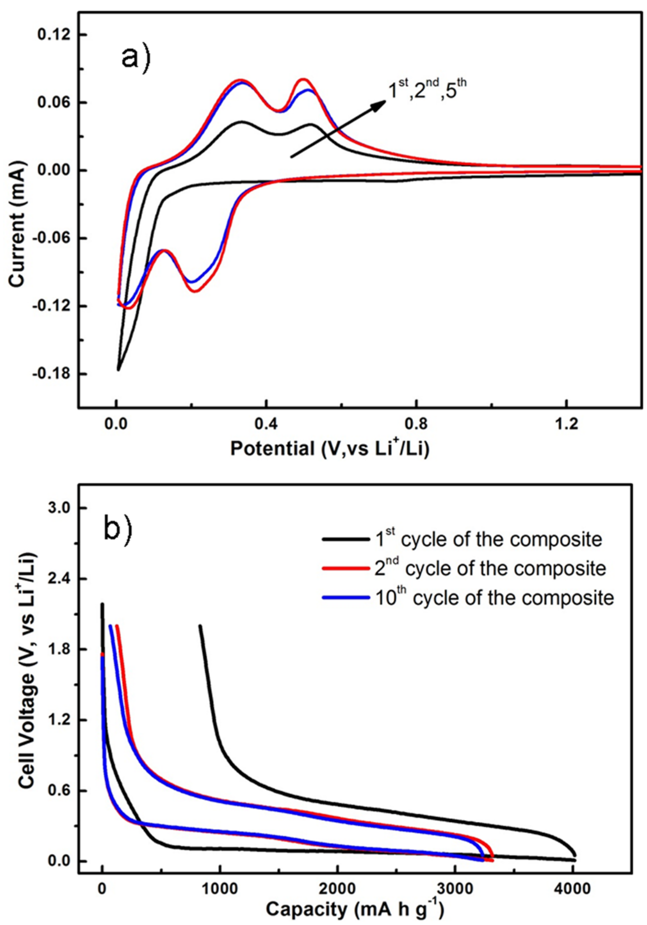

Figure 3. (a) Cyclic voltammograms (CV) and (b) charge/discharge curves of the Si-PPP composite electrode.

Figure 3b displays the typical charge–discharge curves of the composite at a constant current of 300 mA g^{-1}. The initial charge/discharge capacities of the Si-PPP composite are 4015/3184 mA h g^{-1}, with a much higher coulombic efficiency (~78%) than pristine nano-Si electrode (~74%) (see Figure S2 in the Supporting Information). The corresponding volumetric capacity of the Si-PPP composite electrode is calculated to be 2100 mAh cm^{-3}. Herein, a phenomenon worthy of attention is that the PPP polymer electrode only shows a very low coulombic efficiency of ~32% at the first charge and discharge (see Figure S3 in the Supporting Information), but as the shell of the nano-Si particles, this polymer can considerably reduce the initial irreversible capacity loss of the active Si particles in the composite. This fact suggests that the PPP shell can indeed suppress the decomposition of the electrolyte on the Si surface. This is of particular significance for Li-ion battery applications because a large initial capacity loss on the anode must be compensated by excessively loaded cathode.

Figure 4 compares the long-term cyclability of the Si-PPP composite and the pristine nano-silicon anodes at a high current of 3000 mA g^{-1}. To ensure the reproducibility of the result, we assembled two coin cells at a time and simultaneously tested their cycling performance under the same condition. As is clearly seen from Figure 4, the nano-Si anode shows a quite high capacity of 2090 mA h g^{-1} at first cycle, but the reversible capacity falls down very quickly to 1200 mA h g^{-1} in the first 5 cycles and then continuously declines to <200 mA h g^{-1} in subsequent 150 cycles. In contrast, the Si-PPP anode demonstrates a greatly improved cyclability. In addition to its initial high capacity of 2760 mA h g^{-1}, the Si-PPP anode can deliver up to 1820 mA h g^{-1} after 200 cycles and can still retain 1600 mA h g^{-1} even after 400 cycles. At the same time, the coulombic efficiency kept stably at >99% at the prolonged cycles. Similar results are duplicated by another cell.

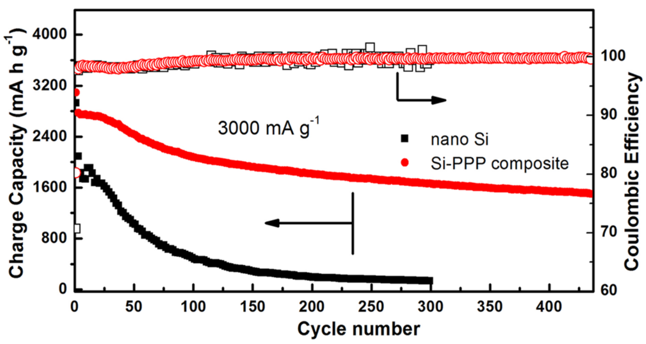

Figure 4. Cycling performance and coulombic efficiency of the pristine nano-silicon and Si-PPP composite electrodes. All the electrodes were cycled at 300 mA g^{-1} for the first cycle, 1500 mA g^{-1} for the second cycle, and 3000 mA g^{-1} for the later cycles.

This Si-PPP electrode has demonstrated not only high reversible capacity and superior cyclability, but also excellent rate capability. As shown in Figure 5, the Si-PPP electrode delivers reversible capacities of 3022 mA h g^{-1} at 300 mA g^{-1}, 2841 mA h g^{-1} at 3 A g^{-1}, and 2415 mA h g^{-1} at 6.0 A g^{-1}. Even at very high rates of 12 and 16 A g^{-1}, the electrode can still deliver considerably high reversible capacities of 2079 and 1670 mA h g^{-1}. In contrast, the pristine nano-Si anode shows a relatively poor rate capability only with a capacity of ~2000 mA h g^{-1} even at a moderate rate of 3 A h g^{-1} (see Figure S4 in the Supporting Information). This comparison demonstrates that the PPP shell can greatly enhance the rate capability of the nano-Si particles.

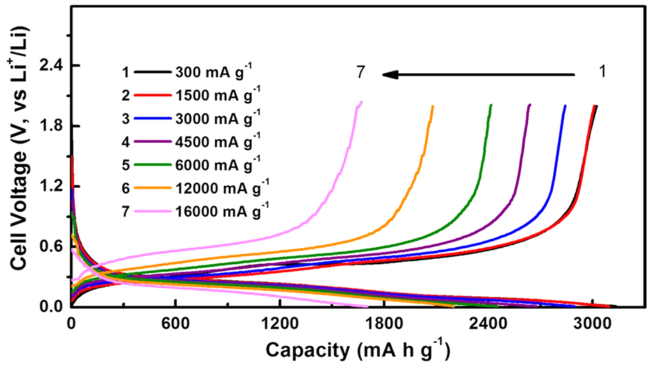

Figure 5. Charge–discharge curves of the Si-PPP composite electrode at various rates from 300 mA g^{-1} to 16000 mA g^{-1}.

The above-presented results clearly demonstrate that the PPP matrix can greatly enhance the electrochemical performance of the nano-Si particles, especially rate capability and long-term cyclability. The enhancing mechanism of the PPP matrix on the nano-Si core may arise from several factors: firstly, the PPP shell can effectively accommodate the volume change and prevent the aggregation of the active Si particles, and therefore increase the mechanical integrity of the electrode. This is confirmed by the TEM image of the Si particle after 20 cycles (see Figure S5 in the Supporting Information). Compared to the uncycled Si particle, the TEM image of the nano-Si after cycling did not show any distinguishable change in morphology and particle size. This structural and morphological stability is no doubt a main cause for the cycling stability of the Si-PPP composite Secondly, the PPP matrix is virtually Li^+- transportable with n-doping activity at more negative potentials, thus enabling Li^+ ions and electrons to arrive at all the nanodomains in the electrode for the alloying reaction. Finally, the PPP shell can separate the nano-Si cores from contact with electrolyte, considerably avoiding the destruction and reconstruction of the SEI film on the Si surface during cycling. To verify this effect, the electrochemical impedance spectra (EIS) of the Si-PPP electrode at different cycles were measured (see Figure S6 in the Supporting Information). As can be seen, the diameter of the semi-circle at the high frequency region, representing the impedance of SEI film, almost remains unchanged during cycling, indicating the stability of the SEI film on the nano-Si surface. Therefore, the stable Si/PPP interfaces are possibly a critical cause for the long-term cyclability of the material.

On the basis of the above results, it seems that a stable electrochemical interface on the nano-Si particles could be established by embedding them into a Li^+-dopable polymer, which provides a fast Li^+ channel for the Li–Si alloy reaction and prevents the contact of electrolyte with the Si surface, thus enabling high capacity utilization, high rate capability, and long-term cycling stability of the Si/polymer composites.

CONCLUSIONS

In summary, we propose a new strategy to construct a cycle-stable Si anode by embedding the nano-Si particles into a Li^+-conductive polymer matrix to prevent the contact of the nano-Si surface with electrolyte, thus suppressing the continual rupturing-reformation of SEI film on the Si surfaces. The thus-prepared Si/PPP composites demonstrated a high capacity of 3184 mA h g^{-1}, a high rate capability of 16 A g^{-1}, and a long-

dx.doi.org/10.1021/am4056672 | ACS Appl. Mater. Interfaces 2014, 6, 3508–3512

term cyclability with 60% capacity retention over >400 cycles, which exceed greatly the electrochemical performances of conventional Si anodes. In addition, the synthetic route developed in this work is facile and easily extendable to other Li-storable metals or alloys for development of advanced anode materials of Li-ion batteries.

■ ASSOCIATED CONTENT

Ⓢ Supporting Information

FTIR spectra of PPP and Si-PPP composite, the charge/discharge curves of the pristine nano-Si electrode and PPP electrode, TEM image of the Si-PPP composite after 20 cycles, and the electrochemical impedance spectra (EIS) of the Si-PPP composite electrode at 20th, 60th, and 100th cycles. This material is available free of charge via the Internet at http://pubs.acs.org.

■ AUTHOR INFORMATION

Corresponding Author

*E-mail: xpai@whu.edu.cn. Phone: +86-27-68754526.

Notes

The authors declare no competing financial interest.

■ ACKNOWLEDGMENTS

This work was financially supported by the National High-tech R&D Program of China (2011AA11A254, 2012AA110102, 2012AA052201), and the National Science Foundation of China (21373154).

■ REFERENCES

(1) Goodenough, J. B.; Park, K. S. The Li-Ion Rechargeable Battery: A Perspective. *J. Am. Chem. Soc.* **2013**, *135*, 1167−1176.
(2) Liu, J.; Zhang, J.-G.; Yang, Z.; Lemmon, J. P.; Imhoff, C.; Graff, G. L.; Li, L.; Hu, J.; Wang, C.; Xiao, J.; Xia, G.; Viswanathan, V. V.; Baskaran, S.; Sprenkle, V.; Li, X.; Shao, Y.; Schwenzer, B. Materials Science and Materials Chemistry for Large Scale Electrochemical Energy Storage: From Transportation to Electrical Grid. *Adv. Funct. Mater.* **2013**, *23*, 929−946.
(3) Choi, N.-S.; Chen, Z.; Freunberger, S. A.; Ji, X.; Sun, Y.-K.; Amine, K.; Yushin, G.; Nazar, L. F.; Cho, J.; Bruce, P. G. Challenges Facing Lithium Batteries and Electrical Double-Layer Capacitors. *Angew. Chem. Int. Ed.* **2012**, *51*, 9994−10024.
(4) Dunn, B.; Kamath, H.; Tarascon, J.-M. Electrical Energy Storage for the Grid: A Battery of Choices. *Science* **2011**, *334*, 928−935.
(5) Yang, Z. G.; Zhang, J. L.; Kintner-Meyer, M. C. W.; Lu, X. C.; Choi, D. W.; Lemmon, J. P.; Liu, J. Electrochemical Energy Storage for Green Grid. *Chem. Rev.* **2011**, *111*, 3577−3613.
(6) Szczech, J. R.; Jin, S. Nanostructured Silicon for High Capacity Lithium Battery Anodes. *Energy Environ. Sci.* **2011**, *4*, 56−72.
(7) Hatchard, T. D.; Dahn, J. R. In situ XRD and electrochemical study of the reaction of lithium with amorphous silicon. *J. Electrochem. Soc.* **2004**, *151*, A838−A842.
(8) Wu, H.; Cui, Y. Designing Nanostructured Si anodes for High Energy Lithium-Ion Batteries. *Nano Today* **2012**, *7*, 414−429.
(9) Chan, C. K.; Peng, H. L.; Liu, G.; McIlwrath, K.; Zhang, X. F.; Huggins, R. A.; Cui, Y. High-Performance Lithium Battery Anodes Using Silicon Nanowires. *Nat. Nanotechnol.* **2008**, *3*, 31−35.
(10) Kim, H.; Seo, M.; Park, M. H.; Cho, J. A Critical Size of Silicon Nano-Anodes for Lithium Rechargeable Batteries. *Angew. Chem., Int. Ed.* **2010**, *49*, 2146−2149.
(11) Lee, J.-I.; Lee, K. T.; Cho, J.; Kim, J.; Choi, N.-S.; Park, S. Chemical-Assisted Thermal Disproportionation of Porous Silicon Monoxide into Silicon-Based Multicomponent Systems. *Angew. Chem., Int. Ed.* **2012**, *51*, 2767−2771.
(12) Zhou, X. S.; Yin, Y. X.; Wan, L. J.; Guo, Y. G. Self-Assembled Nanocomposite of Silicon Nanoparticles Encapsulated in Graphene through Electrostatic Attraction for Lithium-Ion Batteries. *Adv. Energy Mater.* **2012**, *2*, 1086−1090.
(13) Xue, L.; Xu, G.; Li, Y.; Li, S.; Fu, K.; Shi, Q.; Zhang, X. Carbon-Coated Si Nanoparticles Dispersed in Carbon Nanotube Networks As Anode Material for Lithium-Ion Batteries. *ACS Appl. Mater. Interfaces* **2012**, *5*, 21−25.
(14) Gauthier, M.; Mazouzi, D.; Reyter, D.; Lestriez, B.; Moreau, P.; Guyomard, D.; Roue, L. A Low-Cost and High Performance Ball-Milled Si-Based Negative Electrode for High-Energy Li-Ion Batteries. *Energy Environ. Sci.* **2013**, *6*, 2145−2155.
(15) Yao, Y.; Liu, N.; McDowell, M. T.; Pasta, M.; Cui, Y. Improving the Cycling Stability of Silicon Nanowire Anodes with Conducting Polymer Coatings. *Energy Environ. Sci.* **2012**, *5*, 7927−7930.
(16) Memarzadeh, E. L.; Kalisvaart, W. P.; Kohandehghan, A.; Zahiri, B.; Holt, C. M. B.; Mitlin, D. Silicon Nanowire Core Aluminum Shell Coaxial Nanocomposites for Lithium Ion Battery Anodes Grown with and without a TiN Interlayer. *J. Mater. Chem.* **2012**, *22*, 6655−6668.
(17) Liu, X. H.; Fan, F.; Yang, H.; Zhang, S.; Huang, J. Y.; Zhu, T. Self-Limiting Lithiation in Silicon Nanowires. *ACS Nano* **2013**, *7*, 1495−1503.
(18) Liu, X. H.; Zhong, L.; Huang, S.; Mao, S. X.; Zhu, T.; Huang, J. Y. Size-Dependent Fracture of Silicon Nanoparticles During Lithiation. *ACS Nano* **2012**, *6*, 1522−1531.
(19) Magasinski, A.; Dixon, P.; Hertzberg, B.; Kvit, A.; Ayala, J.; Yushin, G. High-Performance Lithium-Ion Anodes Using a Hierarchical Bottom-up Approach. *Nat. Mater.* **2010**, *9*, 353−358.
(20) Wu, H.; Yu, G.; Pan, L.; Liu, N.; McDowell, M. T.; Bao, Z.; Cui, Y. Stable Li-Ion Battery Anodes by in-Situ Polymerization of Conducting Hydrogel to Conformally Coat Silicon Nanoparticles. *Nat. Commun.* **2013**, *4*, 1943.
(21) Kong, J.; Yee, W. A.; Wei, Y.; Yang, L.; Ang, J. M.; Phua, S. L.; Wong, S. Y.; Zhou, R.; Dong, Y.; Li, X.; Lu, X. Silicon Nanoparticles Encapsulated in Hollow Graphitized Carbon Nanofibers for Lithium Ion Battery Anodes. *Nanoscale* **2013**, *5*, 2967−2973.
(22) Piper, D. M.; Yersak, T. A.; Son, S.-B.; Kim, S. C.; Kang, C. S.; Oh, K. H.; Ban, C.; Dillon, A. C.; Lee, S.-H. Conformal Coatings of Cyclized-PAN for Mechanically Resilient Si nano-Composite Anodes. *Adv. Energy Mater.* **2013**, 3, 697−702.
(23) Wu, H.; Chan, G.; Choi, J. W.; Ryu, I.; Yao, Y.; McDowell, M. T.; Lee, S. W.; Jackson, A.; Yang, Y.; Hu, L. B.; Cui, Y. Stable Cycling of Double-Walled Silicon Nanotube Battery Anodes through Solid-Electrolyte Interphase Control. *Nat. Nanotechnol.* **2012**, *7*, 309−314.
(24) Song, T.; Xia, J.; Lee, J.-H.; Lee, D. H.; Kwon, M.-S.; Choi, J.-M.; Wu, J.; Doo, S. K.; Chang, H.; Park, W. I.; Zang, D. S.; Kim, H.; Huang, Y.; Hwang, K.-C.; Rogers, J. A.; Paik, U. Arrays of Sealed Silicon Nanotubes As Anodes for Lithium Ion Batteries. *Nano Lett.* **2010**, *10*, 1710−1716.
(25) Park, M.-H.; Kim, M. G.; Joo, J.; Kim, K.; Kim, J.; Ahn, S.; Cui, Y.; Cho, J. Silicon Nanotube Battery Anodes. *Nano Lett.* **2009**, *9*, 3844−3847.
(26) Novák, P.; Müller, K.; Santhanam, K. S. V.; Haas, O. Electrochemically Active Polymers for Rechargeable Batteries. *Chem. Rev.* **1997**, *97*, 207−282.
(27) Zhu, L. M.; Lei, A. W.; Cao, Y. L.; Ai, X. P.; Yang, H. X. An all-organic rechargeable battery using bipolar polyparaphenylene as a redox-active cathode and anode. *Chem. Commun.* **2013**, *49*, 567−569.
(28) Kovacic, P.; Kyriakis, A. Polymerization of Benzene to *p*-Polyphenyl by Aluminum Chloride-Cupric Chloride. *J. Am. Chem. Soc.* **1963**, *85*, 454−458.
(29) Obrovac, M. N.; Krause, L. J. Reversible Cycling of Crystalline Silicon Powder. *J. Electrochem. Soc.* **2007**, *154*, A103−A108.